



Potential use of shell biomass (*Juglans regia* L.) for dye removal: Relationships between pseudo-second-order kinetic model parameters and biosorption efficiency

Fatih Deniz

Nigar Erturk Trade Vocational High School, 27590 Gaziantep, Turkey
Tel. +90 342 3291194; Fax: +90 342 3291529; email: f_deniz@windowslive.com

Received 28 January 2013; Accepted 8 March 2013

ABSTRACT

The capability of walnut shell for dye removal from aqueous media was investigated and Maxilon Red GRL (MR GRL) was used as a model dye. The pseudo-second-order kinetic model showed the best correlation with the experimental data. The relationships between this kinetic model parameters and biosorption performance were evaluated. The approaching equilibrium factor (R_w) displayed that the biosorption nearly reached equilibrium and approach to equilibrium increased with higher biosorbent dosage. The equilibrium data presented an excellent fit to the Langmuir isotherm model. Thermodynamic analysis proved a spontaneous, favorable, and endothermic process. It can be concluded that walnut shell could be a potential low-cost biosorbent for the MR GRL removal from aqueous solutions.

Keywords: Walnut shell; Dye removal; Kinetic parameters; Biosorption performance

1. Introduction

The pollution control is one of the prime concerns of society today. Untreated or partially-treated wastewaters including dyes from various industrial effluents into natural ecosystems pose a serious problem to the environment. Synthetic dyes have complex aromatic structures which are widely used in the industries such as textiles, rubber, paper, plastics, food, and cosmetics to color their products [1]. These dyes are harmful to fauna, flora, and some of dyes and their products have a mutagenic or carcinogenic influence on human beings [2]. Even at low concentrations, dyes could be highly noticeable, and can cause an esthetic pollution and disturbance to the ecosystem and water sources [3]. Hence, removal of these compounds from the effluents is necessary.

There are many methods like coagulation, chemical oxidation, electrochemical treatments, and membrane technologies to remove dyes from wastewaters. However, these techniques are not very successful due to some restrictions [4]. On the other hand, biosorption is a very effective separation method, and now it is noted to be superior to other techniques for the water treatment with regard to cost economics, eco-compatibility, high efficiency, simplicity of design, ease of operation, and insensitive to toxic substances [5]. Dye removal by activated carbon is a common practice, but its high production cost and regeneration difficulty limit its frequent usage [6]. Therefore, there is a growing interest to search for alternative materials being relatively cost effective and at the same time having high removal efficiency. Herein, the use of

natural biomaterials is a promising alternative due to their relative abundance and low commercial value.

According to FAOSTAT for 2010 year, approximately 846,059 hectares of walnut trees (*Juglans regia* L.) were grown commercially with an estimated annual production of 2,545,388 metric tons of walnut fruits in the world [7]. The major producers of walnut are China, the USA, Iran, and Turkey. Walnut is a round, single-seeded stone fruit of walnut tree. Walnut shell makes up a large percentage of walnut fruit (approximately 50%), and is available in abundant supply as an agricultural by-product of walnut-processing industry. Walnut shell is a hard, chemically inert, nontoxic, and biodegradable material. This shell is also advantageous due to its availability as a renewable resource [8]. A few studies have been reported on the utilization of walnut shell (modified or activated carbon forms) in removing heavy metal ions like mercury, chromium, and lead. But, to my knowledge, this is the first study on the removal capability of raw walnut shell for certain dye.

The goal of this paper is to examine the feasibility of walnut shell for removal of Maxilon Red GRL (MR GRL) from aqueous solutions. The dye was used as a model compound of azo dyes which represent more than a half of the global dye production [9]. Due to the harmful impacts of such dyes, it is environmentally important to remove them from waste streams before discharging to public water sources. The pseudo-first-order, pseudo-second-order, and intraparticle diffusion models were used for analyzing the kinetic data. The relationships between kinetic parameters and biosorption performance at different biosorbent doses were interpreted. The equilibrium data were tested by the Langmuir, Freundlich, and Dubinin–Radushkevich isotherm models. Thermodynamic parameters were also defined for explaining the nature of biosorption process. These studies can provide valuable reference for further dye biosorption researches of walnut shell.

2. Materials and methods

2.1. Preparations of biosorbent and dye solution

Walnut shell was collected from a local source in vicinity of Gaziantep, Turkey. General properties of walnut shell are given in Table 1 [10,11]. The shell was washed several times with distilled water to remove soluble impurities, and this was followed by drying at 80°C for 24 h. The dried biomass was powdered and sieved to obtain particle size range of 63–125 µm. It was then stored in an airtight plastic

Table 1
General properties of walnut shell

Cellulose (%)	23.55
Hemicellulose (%)	29.28
Lignin (%)	37.14
C (%)	48.07
H (%)	7.11
O (%)	42.84
Porosity (%)	52.00
BET surface area (m ² g ⁻¹)	2.79
Surface functional groups (meq g ⁻¹)	–
Basic	0.52
Carboxylic	0.45
Lactonic	0.49
Phenolic	0.39
Total acidic	1.33

container to use as a biosorbent without any pretreatments for biosorption studies.

MR GRL was supplied by a local textile plant. It was of commercial quality and used without further purification. Some characteristics of this dye are presented in Table 2 [12]. A stock solution of 500 mg L⁻¹ was prepared by dissolving accurately weighed quantity of the dye in distilled water. The working solutions of desired concentration were obtained by further dilution from the stock solution. About 0.1 M NaOH and HCl solutions were used for initial pH adjustment.

2.2. Biosorption studies

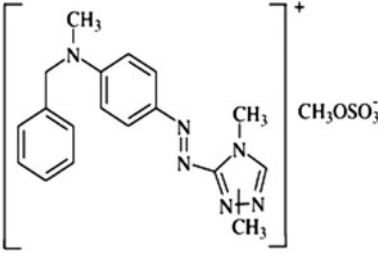
Batch experiments were conducted with different biosorbent doses from 1 to 5 g L⁻¹ at pH 8 and initial dye concentration of 80 mg L⁻¹ in 100 mL Erlenmeyer flasks with 50 mL of the total working volume. The flasks were then agitated at a constant speed in a water bath at 45°C for the required time period. A portion of the samples was collected at regular intervals and centrifuged. The equilibrium concentration of dye was determined by a UV-Vis spectrophotometer at 530 nm.

The amount of dye sorbed onto biosorbent, q (mg g⁻¹), was determined by Eq. (1).

$$q = \frac{(C_o - C_t)V}{M} \quad (1)$$

where C_o is the initial dye concentration (mg L⁻¹), C_t is the residual dye concentration at any time (mg L⁻¹), V is the volume of solution (L), and M is the mass of biosorbent (g). q and C_t are equal to q_e and C_e at equilibrium, respectively.

Table 2
Some characteristics of MR GRL dye

Type	Cationic
λ_{\max} (nm)	530
M_f	$C_{18}H_{24}N_6O_4S$
M_w (g mol ⁻¹)	322
Azo group	1
C.I. name	Basic Red 46
C.I. number	110825
CAS number	12221-69-1
Molecular structure	

2.3. Statistical analysis

Biosorption studies were performed in duplicates for ensuring the reliability and reproducibility of the results obtained, and only the mean values were reported. All the model parameters were determined by linear regression using the Excel 2010 program (Microsoft Co., USA). In addition to the coefficient of determination (R^2), the Chi-square (χ^2) statistical test method was also used to evaluate the best-fit of the model to the experimental data using Eq. (2).

$$\chi^2 = \sum_{i=1}^n \frac{(q_{e,\text{exp}} - q_{e,\text{cal}})^2}{q_{e,\text{cal}}} \quad (2)$$

where n is the number of data points, $q_{e,\text{exp}}$ is the observation from the experiment, and $q_{e,\text{cal}}$ is the calculation from the models. The smaller χ^2 value denotes the best curve fitting.

3. Results and discussion

3.1. Kinetic tests

Kinetics studies provide valuable data for exhibiting the mechanism of biosorption reaction, and predict the rate at which a pollutant is removed from aqueous solutions. In order to investigate the mechanism of MR GRL biosorption onto walnut shell, the pseudo-first-order [13] and pseudo-second-order [14] models were employed using Eqs. (3) and (4), respectively.

$$\frac{1}{q_t} = \frac{1}{q_e} + \frac{k_1}{q_e t} \quad (3)$$

$$\frac{t}{q_t} = \frac{1}{k_2 q_e^2} + \frac{t}{q_e} \quad (4)$$

Also, the initial biosorption rate, h (mg g⁻¹ min⁻¹), is defined by Eq. (5).

$$h = k_2 q_e^2 \quad (5)$$

where k_1 is the constant of pseudo-first-order rate (min⁻¹), k_2 (g mg⁻¹ min⁻¹) is the pseudo-second-order rate constant, and q_e and q_t (mg g⁻¹) are the amounts of dye sorbed at equilibrium and at time t , respectively. The values of k_1 and q_e can be obtained from the intercept and slope of the plots of $1/q_t$ against $1/t$ (Fig. 1(a)) for the pseudo-first-order model while k_2 and q_e values can be calculated from the slope and intercept of the plots of t/q_t vs. t (Fig. 1(b)) for the pseudo-second-order model. Table 3 presents the kinetic model parameters determined with the statistical analysis values. The low R^2 and high χ^2 values for the pseudo-first-order model indicate that the model was not suitable for defining the biosorption kinetics. Contrary to this kinetic model, the biosorption process was well described by the pseudo-second-order model with better statistical results for all biosorbent dosages. Thus, the results suggest that the pseudo-second-order model could be applied effectively for describing the whole dye biosorption process.

The pseudo-first-order and pseudo-second-order models could not elucidate the biosorption diffusion mechanism. Thus, the effect of diffusion as the rate-controlling step in the biosorption was evaluated by the intraparticle diffusion model using Eq. (6) [15].

$$q_t = k_p t^{1/2} + C \quad (6)$$

where k_p is the intraparticle diffusion rate constant (mg g⁻¹ min^{-1/2}) and C (mg g⁻¹) is a constant providing information about the thickness of boundary layer, which can be determined from the intercept and slope of the plots of q_t vs. $t^{1/2}$ (Fig. 1(c)). According to this model, if the plot of q_t vs. $t^{1/2}$ gives a straight line passing through the origin, then the biosorption process is controlled by the intraparticle diffusion, while, if the data exhibit multilinear plots, then two or more steps influence the process. The plots for the MR GRL removal by walnut shell at different biosorbent dosages were multimodal with three distinct regions. The initial curved region corresponds to the external surface sorption, in which the dye diffuses through the

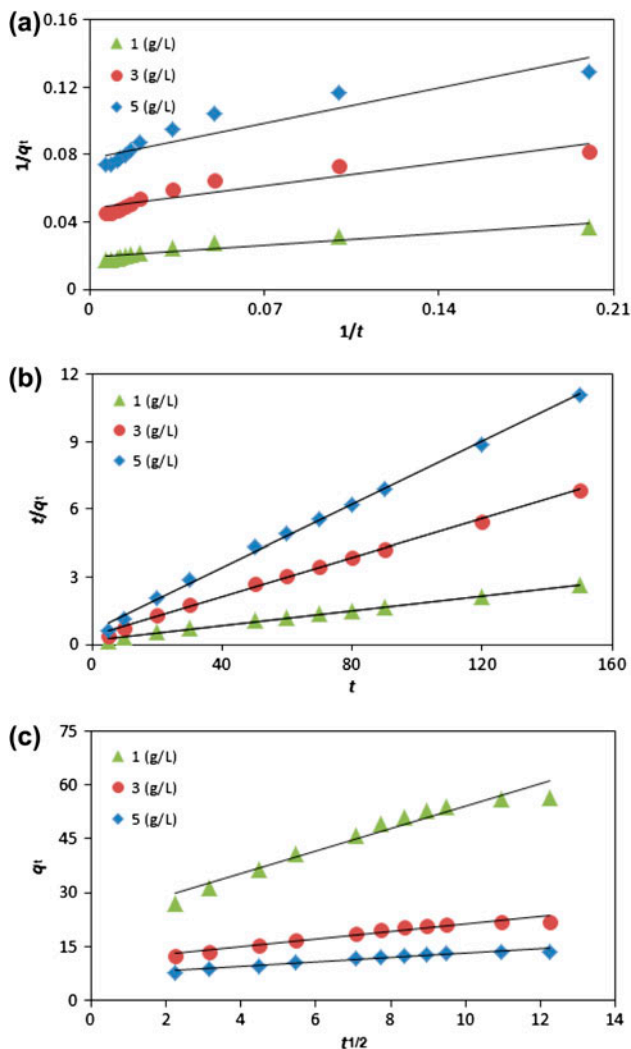


Fig. 1. Plots for biosorption kinetic models employed.

solution to the external surface of biosorbent. The second stage relates the gradual sorption reflecting intraparticle diffusion as the rate-limiting step. The final plateau region points out the surface sorption and the equilibrium stage, in which the intraparticle diffusion starts to slow down and level out [16,17]. This proposes that the biosorption process was rather complex, and involved more than one diffusive resistance.

3.2. Relationships between kinetic parameters and biosorption performance

Recently, Wu et al. [18] have presented a relationship called the approaching equilibrium factor (R_w) between the pseudo-second-order kinetic model parameters and the characteristic kinetic curve. The R_w relationship can be given by Eq. (7).

$$R_w = \frac{1}{1 + k_2 q_e t_w} \quad (7)$$

where t_w (min) is the longest operation time based on kinetic experiments in a biosorption system. A family of curves for $R_w = 0.01$ – 1.00 can then be produced. When $R_w = 1$, the kinetic curve is called linear (zone 0). The possible causes of this effect are: (i) it does not facilitate biosorption when the pseudo-second-order rate constant (k_2) is very small, (ii) the equilibrium amount of biosorption (q_e) is very small, and (iii) the longest operation time (t_w) of biosorption process is too short. All these factors display an ineffective biosorption system, where equilibrium cannot be reached. The curvature of biosorption curve increases as R_w reduces. The characteristic biosorption curve is called approaching equilibrium in the range $1 > R_w > 0.1$ (zone I); called well-approaching equilibrium in the range $0.1 > R_w > 0.01$ (zone II); and called drastically approaching equilibrium when $R_w < 0.01$ (zone III).

The values of R_w defined for the biosorption of MR GRL by walnut shell at different biosorbent doses are shown in Table 4. The R_w values were found to decrease from 0.072 to 0.055 with an increase in the biosorbent dosage range of 1–5 g L⁻¹. These values for R_w lie in zone II under largely curved and well-approaching equilibrium level. The results indicate that this biosorption process nearly reached equilibrium and the approach to equilibrium increased with higher biosorbent doses.

The other parameter in the pseudo-second-order model that can reflect kinetic performance is the second-order rate index (R_i , min⁻¹) and it can be defined by Eq. (8) [18].

$$R_i = k_2 q_e \quad (8)$$

But, there are some drawbacks with R_w in explaining the biosorption rate. If R_i is employed for describing the rate of a biosorption system, this problem can be avoided. Besides, the half-life of biosorption process, $t_{1/2}$, which is the time for half amount of dye to be removed by biosorbent can be stated by Eq. (9).

$$t_{1/2} = \frac{1}{k_2 q_e} \quad (9)$$

It is evident that R_i ($k_2 q_e$) is the only parameter of Eq. (9). The R_i value is equal to the inverse of half-life of biosorption process expressing the actual meaning of second-order biosorption parameter better. The values of R_i obtained for this work are displayed in Table 4. The R_i value increased from 0.086 to

Table 3
Kinetic model parameters obtained with statistical test data

Model	Parameter	Biosorbent dosage (g L ⁻¹)		
		1	3	5
	$q_{e,exp}$ (mg g ⁻¹)	56.29	21.93	13.56
Pseudo-first-order	k_1 (min ⁻¹)	5.4362	4.0291	3.8316
	$q_{e,cal}$ (mg g ⁻¹)	53.19	20.79	12.85
	R^2	0.8956	0.8713	0.8680
	χ^2	4.49	4.68	4.83
Pseudo-second-order	k_2 (g mg ⁻¹ min ⁻¹)	0.0014	0.0048	0.0081
	$q_{e,cal}$ (mg g ⁻¹)	60.24	23.15	14.29
	h (mg g ⁻¹ min ⁻¹)	5.195	2.565	1.651
	R^2	0.9963	0.9974	0.9976
	χ^2	0.75	0.67	0.64
Intraparticle diffusion	k_p (mg g ⁻¹ min ^{-1/2})	3.1311	1.0456	0.6281
	C (mg g ⁻¹)	22.70	10.76	6.84
	R^2	0.9536	0.9511	0.9508
	χ^2	2.78	2.83	2.85

0.116 min⁻¹ with rise in the biosorbent dose from 1 to 5 g L⁻¹. Conversely, the half-life of biosorption process ($t_{1/2}$) has opposite trend as depicted in Table 4. These finding discloses that biosorption half-life shortened with higher biosorbent dosages.

Lastly, based on the pseudo-second-order kinetics, another relationship between operating time required and biosorption amount which is a significant factor in real applications can be described by Eq. (10) [18].

$$t_x = \frac{W}{k_2 q_e} \quad (10)$$

where $W = q_t / (q_e - q_t)$. The fractional biosorption (X) is defined as $X = q_t / q_e$ and $W = X / (1 - X)$. At equilibrium, $q_t / q_e = 1$, $W = \infty$, and $t_x = \infty$. As X equals 1, W approaches infinite. When X is gradually approaching 1, W and t_x increases rapidly. For this study, Table 4 indicates the needed operating times (t_x , min) for different fractional biosorption values (X). For example, the values of $t_{0.60}$ and $t_{0.90}$ for 5 g L⁻¹ biosorbent dose were found to be 12.981 and 77.889 min, respectively. In this case, fractional biosorption value increased from 0.60 to 0.90, the amount of biosorption increased by 50% and the operating time showed a 64.908-min increase. This might be an agreeable variation. On the other hand, for the same biosorbent dosage, the operating time was found to rise from 77.889 to 279.822 min with an increase in fractional biosorption value from 0.90 to 0.97. However, the biosorption amount increased by 7% only,

and the operating time showed a 201.993-min rise. Thence, the researchers should specify the most suitable fractional biosorption value and operating time based on actual working conditions from economic aspect.

3.3. Isotherm analyses

Biosorption isotherm defines the equilibrium relation between pollutant (e.g. dye) amount on biosorbent and its amount in solution, and provides some insight into the biosorption process mechanism and affinity and surface properties of biosorbent. Hence, the Freundlich [19] and Langmuir [20] isotherm mod-

Table 4
Relationships between pseudo-second-order kinetic model parameters and biosorption performance

Parameter	Biosorbent dosage (g L ⁻¹)		
	1	3	5
R_w	0.072	0.057	0.055
R_i (min ⁻¹)	0.086	0.111	0.116
$t_{1/2}$ (min)	11.596	9.023	8.654
$X = 0.60$ $t_{0.60}$	17.395	13.535	12.981
$X = 0.70$ $t_{0.70}$	27.058	21.054	20.193
$X = 0.80$ $t_{0.80}$	46.386	36.093	34.617
$X = 0.90$ $t_{0.90}$	104.367	81.208	77.889
$X = 0.95$ $t_{0.95}$	220.331	171.440	164.431
$X = 0.97$ $t_{0.97}$	374.950	291.748	279.822

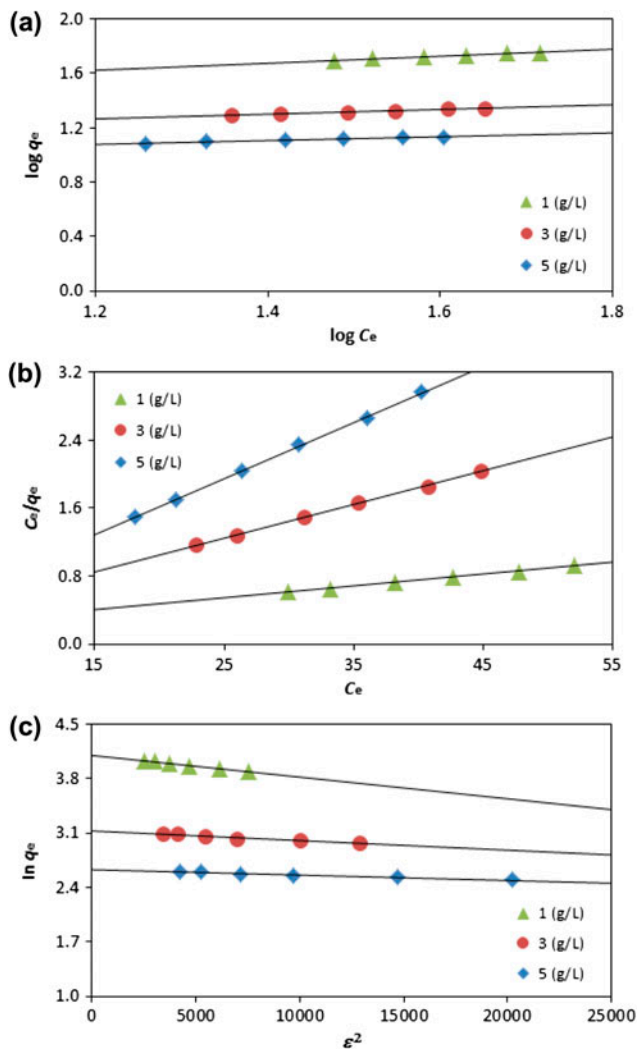


Fig. 2. Plots for equilibrium isotherm models used.

els are employed to illustrate the biosorption equilibrium using Eqs. (11) and (12), respectively.

$$\log q_e = \ln K_f + \frac{1}{n_f} \log C_e \quad (11)$$

$$\frac{C_e}{q_e} = \frac{1}{b q_m} + \frac{C_e}{q_m} \quad (12)$$

Besides, for the Langmuir-type biosorption system, the effect of isotherm shape on whether a biosorption process is favorable or unfavorable can be predicted by the separation factor (R_L , dimensionless) using Eq. (13) [1].

$$R_L = \frac{1}{1 + b C_0} \quad (13)$$

where K_f (mg g^{-1}) (L g^{-1}) $^{1/n}$ is a constant representing the biosorption capacity, n_f is a parameter reflecting the intensity of biosorption, b (L mg^{-1}) is a constant related to the biosorption energy, and q_m is the maximum biosorption capacity (mg g^{-1}). K_f and n_f values can be determined from the slope and intercept of the plots between $\log q_e$ and $\log C_e$ (Fig. 2 (a)) for the Freundlich model, while the values of b and q_m can be calculated from the slope and intercept of the plots between C_e/q_e and C_e (Fig. 2(b)) for the Langmuir model. The isotherm models parameters obtained along with the statistical data are displayed in Table 5. According to the statistical analyses, the Freundlich isotherm model showed very poor fit for the experimental data. Unlike the Freundlich model, the biosorption equilibrium fitted very well to the Langmuir model. This suggests that the biosorption was the monolayer coverage of dye on the biosorbent and the homogeneity of binding sites on the surface of biosorbent [2]. On the other hand, the R_L values between 0 and 1 indicate a favorable biosorption [5]. In the present study, the values of R_L were in the range of 0.07–0.22 showing that the biosorption was favorable. The magnitude of n_f (between 1 and 10) also grants a measure of the conformity of biosorption [16]. The n_f values for this work were in the range of 3.91–7.05 presenting a favorable biosorption.

Table 6 presents the comparison of maximum biosorption capacities of various biosorbents including walnut shell for the MR GRL removal. Walnut shell has higher biosorption capacity for the dye in comparison with many of the other reported biosorbents. In this way, it can be employed as a promising biosorbent for the removal of MR GRL.

The Freundlich and Langmuir isotherm models could not elucidate clearly the type of biosorption behavior (physical or chemical). So, the equilibrium data were further tested by the Dubinin–Radushkevich (D–R) model using Eq. (14) [21].

$$\ln q_e = \ln q_m - B \varepsilon^2 \quad (14)$$

where B is a parameter related to the energy of biosorption and ε is the Polanyi potential. The values of q_m and B can be determined from the slope and intercept of the plots of $\ln q_e$ vs. ε^2 (Fig. 2(c)). The biosorption type based on the D–R model can be predicted by the mean free energy (E , kJ mol^{-1}) employing Eq. (15) [5].

Table 5
Equilibrium isotherm models parameters defined along with statistical analysis values

Model	Parameter	Biosorbent dosage (g L ⁻¹)		
		1	3	5
	$q_{e,exp}$ (mg g ⁻¹)	56.29	21.93	13.56
Freundlich	K_f (mg g ⁻¹) (L g ⁻¹) ^{1/n}	20.69	11.47	8.09
	n_f	3.91	5.80	7.05
	R^2	0.9795	0.9795	0.9828
	χ^2	1.86	1.85	1.65
Langmuir	b (L mg ⁻¹)	0.043	0.103	0.170
	q_m (mg g ⁻¹)	71.43	25.25	15.11
	R_L	0.22	0.11	0.07
	R^2	0.9976	0.9992	0.9994
	χ^2	0.59	0.42	0.39
Dubinin–Radushkevich	q_m (mg g ⁻¹)	60.45	22.83	13.91
	E (kJ mol ⁻¹)	0.13	0.22	0.27
	R^2	0.9774	0.9740	0.9633
	χ^2	2.12	2.31	2.56

Table 6
Biosorption capacities of various biosorbents for MR GRL removal

Sorbent	q_m (mg g ⁻¹)	Reference
Pine cones	73.53	[24]
Pine leaves	71.94	[25]
Canola hull	49.00	[26]
Princess tree leaf	43.10	[27]
Fir sawdust	20.47	[28]
Beech sawdust	19.24	[28]
Walnut shell	71.43	Present study

Table 7
Thermodynamic parameters determined

Parameter	Temperature (°C)		
	25	35	45
ΔG° (kJ mol ⁻¹)	-0.947	-1.753	-2.795
ΔH° (kJ mol ⁻¹)	-	-	26.544
ΔS° (J mol ⁻¹ K ⁻¹)	-	-	0.092
E_a (kJ mol ⁻¹)	-	-	14.403

$$E = 1/(2B)^{1/2} \quad (15)$$

The values of mean free energy between 8 and 16 kJ mol⁻¹ show chemical sorption while the values lower than 8 kJ mol⁻¹ display physical sorption [16]. For the present study, the E values were in the range

of 0.13–0.27 kJ mol⁻¹. These findings propose that the biosorption process proceeded through physical sorption.

3.4. Thermodynamic studies

Thermodynamic data are very significant for giving information about the spontaneity, feasibility, and nature of biosorption process. The standard Gibbs free energy change (ΔG° , kJ mol⁻¹), standard enthalpy change (ΔH° , kJ mol⁻¹), and standard entropy change (ΔS° , J mol⁻¹ K⁻¹) can be obtained by Eqs. (16) and (17) [2].

$$\Delta G^\circ = -RT \ln K_c \quad (16)$$

$$\ln K_c = \frac{\Delta S^\circ}{R} - \frac{\Delta H^\circ}{RT} \quad (17)$$

where R is the universal gas constant (8.314 J mol⁻¹ K⁻¹), T is the temperature (K), K_c is the distribution coefficient (C_s/C_e) and C_s and C_e are the equilibrium dye concentrations on biosorbent (mg L⁻¹) and in solution (mg L⁻¹), respectively. ΔS° and ΔH° values can be defined from the slope and intercept of the plot of $\ln K_c$ vs. $1/T$. The thermodynamic parameters obtained are reported in Table 7. The negative values of ΔG° display the feasibility and spontaneous nature of the biosorption process. The positive value of ΔH° suggests that the endothermic nature of the biosorption, while the positive value of ΔS° indicates an increase in the freedom degree of the dye mole-

cules [22]. Besides, for this study, the values of ΔG° and ΔH° suggest that the mechanism of the dye biosorption was mainly a physical sorption [23].

Furthermore, the activation energy (E_a , kJ mol^{-1}) for this biosorption process was determined by the Arrhenius equation using Eq. (18) [13].

$$\ln k_2 = \ln A - \frac{E_a}{RT} \quad (18)$$

where k_2 is the constant of the pseudo-second-order rate ($\text{g mg}^{-1} \text{min}^{-1}$) and A is the Arrhenius constant. The E_a value can be calculated from the intercept of the plot of $\ln k_2$ against $1/T$. The bigness of E_a presents an idea about the biosorption type. The value of E_a for the biosorption system was found to be $14.403 \text{ kJ mol}^{-1}$ proposing physical sorption [16]. This result agreed well with that from the D–R isotherm model.

4. Conclusions

It was examined the MR GRL biosorption by walnut shell from aqueous solutions. The pseudo-second order was the best model to represent the biosorption kinetics. The parameters of this kinetic model were employed to define the biosorption performance. The R_w values for the work were found to lie in the zone II under largely curved and well-approaching equilibrium level. The Langmuir isotherm model presented the best fit to the equilibrium data. Thermodynamic tests declared a spontaneous and endothermic process. Thus, the current study proposes that walnut shell could procure an effective technology for MR GRL removal from aqueous media.

References

- [1] Y. Yang, G. Wang, B. Wang, Z. Li, X. Jia, Q. Zhou, Y. Zhao, Biosorption of acid black 172 and congo red from aqueous solution by nonviable *Penicillium* YW 01: Kinetic study, equilibrium isotherm and artificial neural network modeling, *Bioresour. Technol.* 102 (2011) 828–834.
- [2] H.B. Senturk, D. Ozdes, C. Duran, Biosorption of Rhodamine 6G from aqueous solutions onto almond shell (*Prunus dulcis*) as a low cost biosorbent, *Desalination* 252 (2010) 81–87.
- [3] V. Vimonses, B. Jin, C.W.K. Chow, Insight into removal kinetic and mechanisms of anionic dye by calcined clay materials and lime, *J. Hazard. Mater.* 177 (2010) 420–427.
- [4] M.A.M. Salleh, D.K. Mahmoud, W.A.W.A. Karim, A. Idris, Cationic and anionic dye adsorption by agricultural solid wastes: A comprehensive review, *Desalination* 280 (2011) 1–13.
- [5] K.Y. Foo, B.H. Hameed, Insights into the modeling of adsorption isotherm systems, *Chem. Eng. J.* 156 (2010) 2–10.
- [6] P. Sharma, H. Kaur, M. Sharma, V. Sahore, A review on applicability of naturally available adsorbents for the removal of hazardous dyes from aqueous waste, *Environ. Monit. Assess.* 183 (2011) 151–195.
- [7] FAOSTAT, <http://faostat.fao.org>, accessed in August 2012.
- [8] A. Srinivasan, T. Viraraghavan, Removal of oil by walnut shell media, *Bioresour. Technol.* 99 (2008) 8217–8220.
- [9] M. Kousha, E. Daneshvar, H. Dopeikar, D. Taghavi, A. Bhatnagar, Box-Behnken design optimization of Acid Black 1 dye biosorption by different brown macroalgae, *Chem. Eng. J.* 179 (2012) 158–168.
- [10] T. Altun, E. Pehlivan, Removal of Cr(VI) from aqueous solutions by modified walnut shells, *Food Chem.* 132 (2012) 693–700.
- [11] M. Zabihi, A. Haghghi Asl, A. Ahmadpour, Studies on adsorption of mercury from aqueous solution on activated carbons prepared from walnut shell, *J. Hazard. Mater.* 174 (2010) 251–256.
- [12] A. Olgun, N. Atar, Equilibrium and kinetic adsorption study of Basic Yellow 28 and Basic Red 46 by a boron industry waste, *J. Hazard. Mater.* 161 (2009) 148–156.
- [13] Z. Bekçi, Y. Seki, L. Cavas, Removal of malachite green by using an invasive marine alga *Caulerpa racemosa* var. *cylindracea*, *J. Hazard. Mater.* 161 (2009) 1454–1460.
- [14] Y.S. Ho, G. McKay, Pseudo-second order model for sorption processes, *Process Biochem.* 34 (1999) 451–465.
- [15] W.J. Weber, J.C. Morris, Kinetics of adsorption on carbon from solution, *J. Sanit. Eng. Div. ASCE* 89 (1963) 31–60.
- [16] S. Chowdhury, P. Saha, Sea shell powder as a new adsorbent to remove Basic Green 4 (Malachite Green) from aqueous solutions: equilibrium, kinetic and thermodynamic studies, *Chem. Eng. J.* 164 (2010) 168–177.
- [17] P.D. Saha, S. Chakraborty, S. Chowdhury, Batch and continuous (fixed-bed column) biosorption of crystal violet by *Artocarpus heterophyllus* (jackfruit) leaf powder, *Colloid Surface B.* 92 (2012) 262–270.
- [18] F.C. Wu, R.L. Tseng, S.C. Huang, R.S. Juang, Characteristics of pseudo-second-order kinetic model for liquid-phase adsorption: A mini-review, *Chem. Eng. J.* 151 (2009) 1–9.
- [19] H.M.F. Freundlich, Over the adsorption in solution, *J. Phys. Chem.* 57 (1906) 385–470.
- [20] I. Langmuir, The adsorption of gases on plane surfaces of glass, mica and platinum, *J. Am. Chem. Soc.* 40 (1918) 1361–1403.
- [21] M.M. Dubinin, L.V. Radushkevich, Equation of the characteristic curve of activated charcoal, *Proc. Acad. Sci. USSR* 55 (1947) 331–333.
- [22] N.M. Mahmoodi, B. Hayati, M. Arami, Kinetic, equilibrium and thermodynamic studies of ternary system dye removal using a biopolymer, *Ind. Crops Prod.* 35 (2012) 295–301.
- [23] Y. Feng, F. Yang, Y. Wanga, L. Ma, Y. Wua, P.G. Kerr, L. Yang, Basic dye adsorption onto an agro-based waste material - Sesame hull (*Sesamum indicum* L.), *Bioresour. Technol.* 102 (2011) 10280–10285.
- [24] F. Deniz, S. Karaman, S.D. Saygideger, Biosorption of a model basic dye onto *Pinus brutia* Ten.: Evaluating of equilibrium, kinetic and thermodynamic data, *Desalination* 270 (2011) 199–205.
- [25] F. Deniz, S. Karaman, Removal of Basic Red 46 dye from aqueous solution by pine tree leaves, *Chem. Eng. J.* 170 (2011) 67–74.
- [26] N.M. Mahmoodi, M. Arami, H. Bahrami, S. Khorramfar, Novel biosorbent (*Canola* hull): Surface characterization and dye removal ability at different cationic dye concentrations, *Desalination* 264 (2010) 134–142.
- [27] F. Deniz, S.D. Saygideger, Removal of a hazardous azo dye (Basic Red 46) from aqueous solution by princess tree leaf, *Desalination* 268 (2011) 6–11.
- [28] L. Laasri, M. Khalid Elamrani, O. Cherkaoui, Removal of two cationic dyes from a textile effluent by filtration-adsorption on wood sawdust, *Environ. Sci. Poll. Res. Int.* 14 (2007) 237–240.